Generalized Averaging Method for Power Conversion Circuits *

Seth R. Sanders   J. Mark Noworolski
Department of Electrical Engineering
and Computer Sciences
University of California, Berkeley

Xiaojun Z. Liu   George C. Verghese
Laboratory for Electromagnetic
and Electronic Systems
Massachusetts Institute of Technology

Abstract

The method of state-space averaging has been successfully applied to pulse-width modulated power converters, but has its limitations with switched circuits that do not satisfy a "small ripple" condition. This work considers a more general averaging procedure that encompasses state-space averaging and is potentially applicable to a much broader class of circuits and systems. In particular, the technique is shown to be effective on a number of examples including resonant type converters.

1   Introduction

State-space averaging [1, 2, 3] has been demonstrated to be an effective method for analysis and control design in pulse-width modulated (PWM) switching power converters. However, as has been noted in the literature, the class of converters that this method can be applied to is limited. Conditions for the justification of state-space averaging have been characterized by a "small ripple" condition, by a "linear ripple" approximation [1], and by the degree to which certain vector fields commute [2]. With the small ripple approximation, the assumption is that a Fourier series expansion for a finite length segment of a circuit waveform should be dominated by its DC term. The linear ripple approximation requires that the circuit waveforms appear to be linear functions of time when examined over a time interval inbetween switch instances. This condition has been stated more precisely in [2] in terms of the Lie bracket of a pair of matrices. A recent paper [6] studied the application of classical averaging techniques in PWM circuits, and has developed an asymptotic framework where solutions to switched systems may be approximated to arbitrary accuracy by a power series in a small parameter. The small parameter is evidently related to the ratio of the switching period and the system time constants. We note here that this ratio is typically small for fast switching PWM circuits, but this is typically not the case for resonant type converters.

Because of the conditions listed above that limit the applicability of state-space averaging, the method cannot be applied to a wide range of power circuits that includes the resonant type converters. The basic limitation in resonant converters is that these circuits have state variables that exhibit predominantly oscillatory behavior. This paper investigates a more general averaging scheme that can, in principle, accomodate arbitrary types of waveforms. The method is based on a time-dependent Fourier series representation for a "sliding window" of a given waveform. For example, for an arbitrary time-domain waveform $x(\bullet)$, the method considers the Fourier coefficients of $x(s)$ for $s \in (t - T, t]$ at the time instant t. Simplifying approximations can be made by omitting insignificant terms in this series. For instance, to recover the traditional state-space averaged model, one would retain only the DC coefficient in this averaging scheme.

Previously developed methods for analysis and control design in resonant converters have relied mainly on two approaches, sampled-data modeling [4, 5] and phase-plane techniques [7, 8]. The sampled-data approach taken in [4, 5] results in a small-signal model for the underlying resonant converter with the perturbation in switching frequency as the input. One difficulty with this approach is the requirement of obtaining a nominal periodic solution as a first step in the analysis. The utility of the resulting model is then limited by its small signal nature. The phase plane method of [7] is a basic approach to obtaining a steady state solution for a resonant converter, and the control scheme of [8] based on this method is evidently effective. A limitation of this approach is its restriction to second order systems; it is not obvious how one can incorporate additional state variables that are associated with the load or the source dynamics. In contrast, the method presented in this paper is an averaging scheme that can be applied, in principle, to any periodically driven system.

The remainder of the paper is organized as follows. Section 2 reviews some of the main techniques used in analyzing oscillations in nonlinear systems. Our approach is outlined in Section 3 and will be seen to be very closely related to the classical methods discussed in Section 2. Examples of the application of our method in resonant and in PWM converters are presented in Section 4. Appendix A contains some comments on the justification of our scheme.

2   Averaging and Oscillations in Nonlinear Systems

One of the pioneers in the study of oscillations in nonlinear systems was van der Pol [11] who studied a periodically

driven, nonlinearly damped oscillator modeled by

$$\ddot{v} + \phi(v)\dot{v} + \omega_0^2 v = \omega_1^2 B sin(\omega_1 t) \qquad (1)$$

The paper [11] postulated a solution of the form

$$v(t) = b_1(t)sin(\omega_1 t) + b_2(t)cos(\omega_1 t) \qquad (2)$$

where $b_1(t)$ and $b_2(t)$ were supposed to be slowly varying functions of time. That is, for $k = 1, 2$,

$$\dot{b}_k(t) \ll \omega_1 b_k(t) \qquad (3)$$

$$\ddot{b}_k(t) \ll \omega_1 \dot{b}_k(t) \qquad (4)$$

Van der Pol's method proceeds by firstly inserting the postulated solution (2) into (1) and extracting the fundamental harmonic response from the nonlinear element in the model (1). (The extraction of the fundamental harmonic response is known as harmonic linearization and is essentially equivalent to the describing function method described below.) Secondly, harmonic balance is imposed to obtain two equations, one in $sin(\omega_1 t)$ and one in $cos(\omega_1 t)$. The result is a state-space model that governs the behavior of the coefficients $b_1(t)$ and $b_2(t)$. The method to be introduced in Section 3 draws on these ideas, but makes slightly different assumptions.

A similar approach to the study of the second order system (1) was taken in the work of Krylov, Bogoliubov, and Mitropolsky [12]. This work relied on the assumption of slowly varying phase and amplitude, i.e. postulated a solution of the form

$$v(t) = a(t)sin\{\omega_0 t + \theta(t)\} \qquad (5)$$

$$\dot{v}(t) = a(t)\omega_0 cos\{\omega_0 t + \theta(t)\} \qquad (6)$$

where $a(t)$ and $\theta(t)$ were supposed to be slowly varing functions of time. An implicit constraint arising from (5,6) is that

$$\dot{a}(t)sin\{\omega_0 t + \theta(t)\} + a(t)\dot{\theta}(t)cos\{\omega_0 t + \theta(t)\} = 0. \qquad (7)$$

The method of [12] proceeds similarly to van der Pol's technique by substituting the postulated form of solution (5,6) into the nonlinear differential equation (1) to derive a state-space equation for the variables $a(t)$ and $\theta(t)$. The assumption of slowly varying phase and amplitude is used to deduce an averaged model for the evolution of $a(t)$ and $\theta(t)$. The averaging operation performed in the method of [12] is actually equivalent to harmonic linearization in that the fundamental component of the response of the nonlinear element of (1) is extracted. See [12] for more details on this method or the summaries in [10, 13].

Another technique that is closely related to the methods outlined above is the describing function method discussed in detail in Gelb and Vander Velde [13]. This method relies on harmonic balance for analyzing steady state and transient oscillations in nonlinear systems. To understand the method, consider the autonomous system of Figure 1 that has a static nonlinearity $N(\bullet)$ in the feedback path. The input to the nonlinearity is labeled $x(t)$ and the output is

$$y(t) = N\{x(t)\}. \qquad (8)$$

The sinusoidal describing function method is a technique for analyzing limit cycles in a system of the type of Figure 1 or
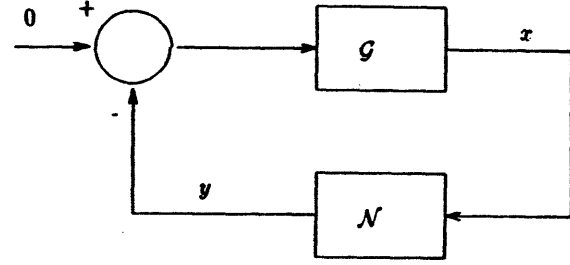

Figure 1: Nonlinear Feedback System

in such a system that has an external periodic input. The basic premise of the describing function method is that $x(t)$ is approximately a sinusoidal waveform, i.e.

$$x(t) \approx X sin(\omega t). \qquad (9)$$

If the nonlinearity is not too severe, that is it does not generate excessively large harmonics, and if the linear transfer function $G(s)$ is a good low pass filter, the assumption that $x(t)$ is sinusoidal is quite plausible. The describing function method characterizes $y(t)$ by its fundamental frequency component

$$y(t) \approx \mathcal{N}(X)x(t) \qquad (10)$$

where $\mathcal{N}(X)$ is the ratio of the fundamental component of $y(t)$ to that of $x(t)$. $\mathcal{N}(X)$ is called the sinusoidal describing function for $N(\bullet)$ and is dependent on the amplitude X of the oscillation. For the loop of Figure 1, the condition for a steady state oscillation is

$$1 + G(j\omega)\mathcal{N}(X) = 0, \qquad (11)$$

or equivalently

$$G(j\omega) = -1/\mathcal{N}(X). \qquad (12)$$

The power of the method is evident from (12) since this equation can be solved graphically by plotting $G(j\omega)$ and $-1/\mathcal{N}(X)$ on the complex plane and determining intersection points of these graphs. Each intersection point (X^*, ω^*) generates a candidate for an approximate limit cycle solution of the form

$$x(t) \approx X^* sin(\omega^* t). \qquad (13)$$

The paper of Bergen and Franks [14] gives conditions under which an exact periodic solution is nearby and gives error bounds on the approximate solution in terms of the operators $G(j\omega)$ and $N(\bullet)$. The describing function method can also be used when periodic external signals enter the system. In this case, one seeks a periodic solution with fundamental frequency equal to the drive frequency. The sinusoidal describing function method generates the amplitude and phase of an approximate solution.

The describing function technique has been generalized for the analysis of transient oscillations in [13]. The generalization assumes a solution of the form

$$x(t) = X(t)e^{j\phi(t)}, \qquad (14)$$

2

which can be identified with the method of slowly varying phase and amplitude [12] if one takes $\phi(t) = \omega_0 t + \theta(t)$. The transient analysis proceeds by noting that

$$\dot{x}(t) = \dot{X}e^{j\phi(t)} + j\dot{\phi}Xe^{j\phi(t)}$$

$$= (\frac{\dot{X}}{X} + j\dot{\phi})Xe^{j\phi(t)} \qquad (15)$$

and identifying these quantities by

$$\dot{x}(t) = (\sigma(t) + j\omega(t))x(t) = sx(t). \qquad (16)$$

Although not clearly stated in [13], the method evidently then replaces $G(j\omega)$ by $G(\sigma + j\omega)$ and imposes harmonic balance by replacing nonlinearities with amplitude-dependent describing functions. The result is a pair of coupled differential equations (corresponding to real and imaginary components) in $\sigma(t),\omega(t)$, and the derivatives of these variables. Reference [13] continues by giving approximate schemes for solving the obtained differential equations. Our method considered in the sequel is closely related to the transient and steady state analysis techniques that rely on describing functions.

3 Generalized Averaging

Our averaging method is based on the fact that the waveform $x(\bullet)$ can be approximated on the interval $(t-T, t]$ to arbitrary accuracy with a Fourier series representation of the form

$$x(t,s) = x(t - T + s) = \sum_k \langle x \rangle_k(t)e^{jk\omega_s(t-T+s)} \qquad (17)$$

where the sum is over all integers k, $\omega_s = 2\pi/T$, $s \in (0,T]$, and the $\langle x \rangle_k(t)$ are complex Fourier coefficients. These Fourier coefficients are functions of time and are determined by

$$\langle x \rangle_k(t) = \frac{1}{T} \int_0^T x(t - T + s)e^{-jk\omega_s(t-T+s)}\, ds. \qquad (18)$$

The k-th coefficient will also be referred to as the index-k coefficient. Note that the strategy here is to consider a window of length T of a given waveform, and to view the waveform as periodic (or having finite duration T) so that it can be analyzed with a Fourier series. The remaining steps in the analysis simply compute the time-evolution of these Fourier series coefficients as the window of length T slides over the actual waveform. Our approach in doing so is to determine an appropriate state-space model in which the coefficients (18) are the states. In this way, the technique is very similar to the classical methods for analyzing nonlinear oscillations.

As an aside, note that one possible approach for deriving the theory of state-space averaging is to consider the one-cycle average

$$\bar{x}(t) = \frac{1}{T} \int_{t-T}^t x(s)\, ds \qquad (19)$$

for the state $x(t)$ of a switching converter operating at frequency $1/T$. The connection with our scheme is that $\bar{x}(t) = \langle x \rangle_0(t)$ corresponds to the DC coefficient in the Fourier series representation (17). More details on this are given Section 4.

Certain properties of the Fourier coefficients (18) are key for the analysis and are detailed below.

Differentiation with respect to time The time derivative of the k-th coefficient is computed to be

$$\frac{d}{dt}\langle x \rangle_k(t) = \left\langle \frac{d}{dt}x \right\rangle_k(t) - jk\omega_s\langle x \rangle_k(t). \qquad (20)$$

This formula will be very important in computing the form of an averaged model involving the Fourier coefficients. The case where ω_s is time varying will also need to be considered for the analysis of systems where the drive frequency is not constant, e.g. in resonant type converters. In this case, the formula (20) is only an approximation, but, for slowly varying $\omega_s(t)$, it is a good approximation. Appendix A gives details on the approximations involved.

Transforms of functions of variables Another important ingredient in the Fourier series coefficient representation of a signal involves the computation of the following:

$$\langle f(x_1, x_2, \ldots, x_n) \rangle_k \qquad (21)$$

where $f(\bullet, \ldots, \bullet)$ is a general scalar function of its arguments. One approach for computing the quantity (21) is by the describing function method [13]. As outlined earlier, this would require the assumption that the arguments $x_1, x_2, \ldots, x_n$ are sinusoidal in nature or perhaps have some other fixed waveshape. For instance, one special case is where it is desired to compute $\langle f(x) \rangle_1$ and $\langle f(x) \rangle_{-1}$, and it is known that x is dominated by its fundamental Fourier components. This would fit the framework of the sinusoidal describing function method. An example of this type is given in Section 4 in the context of a resonant converter.

A procedure for exactly computing (21) is available in the case where $f(\bullet, \ldots, \bullet)$ is polynomial. The procedure is based on the following convolutional relationship:

$$\langle xy \rangle_k = \sum_i \langle x \rangle_{k-i}\langle y \rangle_i \qquad (22)$$

where the sum is taken over all integers i. In many cases, we shall rely on many of the terms in the series in (22) being negligibly small. The quantity in (21) can be computed in the case where $f(\bullet, \ldots, \bullet)$ is a polynomial by considering each homogeneous term separately. The constant and linear terms are trivial to transform. The transforms of the quadratic terms can be computed using (22). Homogeneous terms of higher order can be dealt with by factoring each such term into the product of two lower order terms. Then the procedure can be applied to each of the factors. This process is guaranteed to terminate since factors with only linear terms will eventually arise.

Application to state-space models of power electronic circuits Here we consider the application of the method to a state-space model that has some periodic time-dependence. This is the type of model that typically arises in a switched power electronic circuit. For instance, consider the model

$$\frac{d}{dt}x(t) = f\{x(t), u(t)\} \qquad (23)$$

where $u(t)$ is some periodic function of time with period T. The variable $u(t)$ may be the ramp function used to implement a PWM scheme, or may be a square wave of source voltage applied to a resonant tank circuit in a resonant converter.

To apply the generalized averaging scheme to a converter with model (23), we simply compute the relevant Fourier coefficients of both sides of (23), i.e.

$$\left\langle \frac{d}{dt}x \right\rangle_k = \langle f(x,u) \rangle_k \qquad (24)$$

for the k-th coefficient. A first step in simplifying the model is to incorporate the rule for computing the derivative of the k-th coefficient. We obtain

$$\frac{d}{dt}\langle x \rangle_k = -jk\omega_s \langle x \rangle_k + \langle f(x,u) \rangle_k. \qquad (25)$$

The second term on the right-hand side of (25) can be simplified into explicit functions of the coefficients $\langle x \rangle_i$ and $\langle u \rangle_i$ using describing functions. The essence in modeling is to retain only the relatively large Fourier coefficients to capture the interesting behavior of the system. As previously discussed, we would retain only the index-zero (DC) coefficients for a fast switching PWM circuit to capture the low frequency behavior. The result would be precisely the state-space averaged model. For a resonant converter which has some of its states exhibiting predominantly fundamental frequency, sinusoidal waveforms and some of its states exhibiting predominantly DC (or slowly varying) waveforms, we would retain the index-one (and minus one) coefficients for those states exhibiting sinusoidal-type behavior and the index-zero coefficients for those states exhibiting slowly varying behavior.

The method is demonstrated on some examples in the following section.

4   Examples

Series Resonant Converter with Voltage Source Load
The first example to be considered is the series resonant converter of Figure 2 that has a voltage source load. The circuit parameters are as given in the figure and the diodes are assumed to be ideal. Note that the resonant tank frequency is approximately 36KHz.

A state-space model for this circuit takes the form

$$\frac{d}{dt}i = \frac{1}{L}\{-v - V_o sgn(i) + V_s sgn(sin(\omega_s t))\}$$
$$\frac{d}{dt}v = \frac{1}{C}i \qquad (26)$$

where $sgn(\bullet)$ indicates the sign function. Typical waveforms for this circuit are shown in the figure. These waveforms were generated by stepping the drive frequency between 38KHz and 40KHz. One of the important features of the waveforms is that following each step change in the driving frequency, the waveforms appear to be amplitude modulated sinusoids. The waveforms evidently settle down to an approximately sinusoidal steady state. For this reason, these waveforms may be very well approximated with the fundamental frequency terms in the Fourier series (17). We are led to examine a model containing only the coefficients $\langle i \rangle_1, \langle i \rangle_{-1}, \langle v \rangle_1$, and $\langle v \rangle_{-1}$. This can be obtained by considering the application of the operator $\langle \bullet \rangle_1$ (or equivalently $\langle \bullet \rangle_{-1}$) to the model (26), i.e.
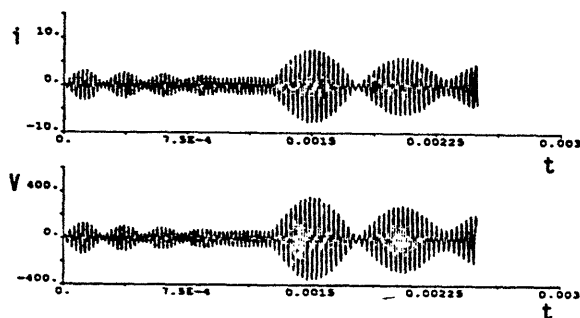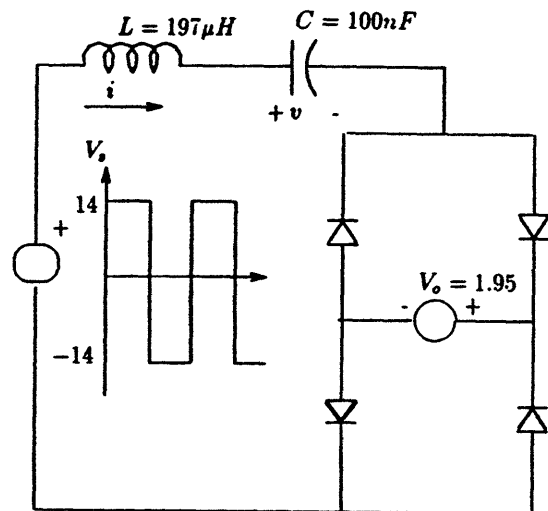

Figure 2:   DC-DC Series Resonant Converter with Voltage Source Load

$$\frac{d}{dt}\langle i \rangle_1 = -j\omega_s \langle i \rangle_1 + \frac{1}{L}\{-\langle v \rangle_1 - V_o \langle sgn(i) \rangle_1 + V_s \langle sgn(sin(\omega_s t)) \rangle_1\}$$
$$\frac{d}{dt}\langle v \rangle_1 = -j\omega_s \langle v \rangle_1 + \frac{1}{C}\langle i \rangle_1 \qquad (27)$$

Note that the elements of the two component state vector of (27) are complex Fourier coefficients, and so this model actually corresponds to a fourth-order state-space model with real variables. The corresponding real fourth-order model could be obtained equivalently from the index-(-1) coefficients. If the window length is taken to be $T = 2\pi/\omega_s$, the term

$$\langle sgn(sin(\omega_s t)) \rangle_1 = -j\frac{2}{\pi} \qquad (28)$$

is simply the constant amplitude of the first coefficient of the Fourier series for a square wave. The term $\langle sgn(i) \rangle_1$ can be evaluated using the describing function approach by assuming

4

$i(t)$ is approximated as a sinusoid over each interval of length T. In this case, we have

$$\langle sgn(i)\rangle_1 = \frac{2}{\pi}e^{j\angle\langle i\rangle_1}. \qquad (29)$$

Consequently, the model (27) is approximated with the time-invariant model

$$\frac{d}{dt}\langle i\rangle_1 = -j\omega_s\langle i\rangle_1 + \frac{1}{L}\{-\langle v\rangle_1 - V_o\frac{2}{\pi}e^{j\angle\langle i\rangle_1} - V_s j\frac{2}{\pi}\}$$

$$\frac{d}{dt}\langle r\rangle_1 = -j\omega_s\langle v\rangle_1 + \frac{1}{C}\langle i\rangle_1. \qquad (30)$$

The variables ω_s and V_s may be considered as external inputs to this model. One question that arises is how well the magnitudes of the complex coefficients

$$\| \langle i\rangle_1 \| = \sqrt{(Re\langle i\rangle_1)^2 + (Im\langle i\rangle_1)^2}$$

$$\| \langle v\rangle_1 \| = \sqrt{(Re\langle v\rangle_1)^2 + (Im\langle v\rangle_1)^2}. \qquad (31)$$

coincide with the amplitude of the waveforms in Figure 2. The simulation of Figure 3 compares precisely these quanti-
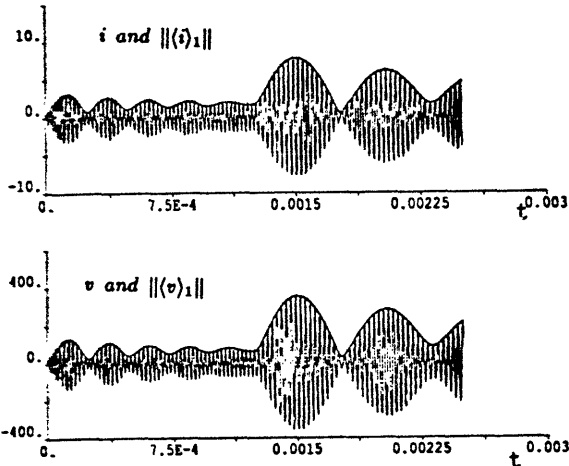

Figure 3: Amplitude of First Coefficients Compared to Actual Waveforms

ties. This figure plots on the same axes the waveforms $v(t)$ and $\|\langle r\rangle_1(t)\|$ for the case where ω_s undergoes a step change, and the figure similarly plots $i(t)$ and $\|\langle i\rangle_1(t)\|$. It is evident from the figure that the correlation between the two types of waveforms is excellent.

The utility of the method can now be realized. For instance, it is straightforward to obtain a steady state solution for this model by setting the derivatives of $\langle v\rangle_1$ and $\langle i\rangle_1$ to zero. This solution can be computed in a closed form. After obtaining a steady state solution, the model may be linearized about the steady state to obtain small signal transfer functions from inputs such as switching frequency ω_s or source voltage V_s to variables such as $\langle v\rangle_1$ or $\langle i\rangle_1$. For purposes of illustration, we carry out this procedure here.

The steady state solution is determined to be

$$\langle v\rangle_1^{ss} = \frac{2}{\pi}\frac{\sqrt{V_s^2 - V_o^2}}{|1 - \omega_s^2 LC|} \qquad (32)$$

$$\langle i\rangle_1^{ss} = j\omega_s C\langle v\rangle_1^{ss}. \qquad (33)$$

By considering perturbations around this steady state solution it is possible to compute the transfer function from input switching frequency ω_s to the capacitor voltage amplitude $\|\langle v\rangle_1\|$. This is given by

$$-M\omega_s\frac{Ks + 2\Delta}{s^4 + Ks^3 + 2\Sigma s^2 + K\Sigma s + \Delta^2} \qquad (34)$$

where $M = \|\langle v\rangle_1^{ss}\|$, $K = 2\omega_0^2 V_o/\pi M\omega_s$, $\omega_0^2 = 1/LC$, $\Sigma = \omega_0^2 + \omega_s^2$, and $\Delta = \omega_s^2 - \omega_o^2$. A root locus of the poles of this transfer function is shown in Figure 4. The plot shows the location of the poles as the load voltage V_o increases from zero to V_s. The poles are seen to be damped for $0 < V_o <$
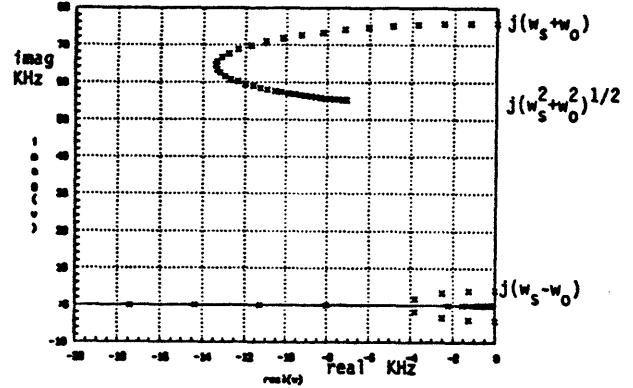

Figure 4: Root Locus of Small Signal Poles as Load Voltage Varies from Zero to V_s

V_s. For small values of V_o, there is a pair of poles located near $\pm j(\omega_s - \omega_0)$. This pair evidently governs the relatively slow amplitude modulation seen in Figure 3. One argument for the presence of this slow amplitude modulation is that it is the result of beating between oscillations at the natural frequency ω_0 and the driving frequency ω_s. Note that the locus of Figure 4 closely resembles the locus of reference [4] that was determined using an "exact" sampled-data model. It is also of interest that the transfer function (34) has a right-half plane zero for $\Delta < 0$, that is for frequencies below resonance.

One interesting feature of the simulation of Figure 3 is that the high frequency modes of the model (34) are not evident in the transient response. This can be attributed to the fact that these modes are weakly coupled to the input corresponding to perturbations in driving frequency ω_s. •

DC-DC Series Resonant Converter with Capacitor Load

A more complex example is the series resonant converter with a capacitor load that is shown in Figure 5. For this example, a state-space model can be written as

$$\frac{d}{dt}i = \frac{1}{L}\{-v - v_o sgn(i) + V_s sgn(sin(\omega_s t))\}$$

$$\frac{d}{dt}v = \frac{1}{C}i$$

$$\frac{d}{dt}v_o = \frac{1}{C_o}\{abs(i) - v_o/R\}. \qquad (35)$$

5

Figure 5: DC-DC Series Resonant Converter with Capacitor Load

Figure 6: Comparison of Transient Waveforms of Avaraged Model with Waveforms of Underlying Resonant Converter with Capacitor Load
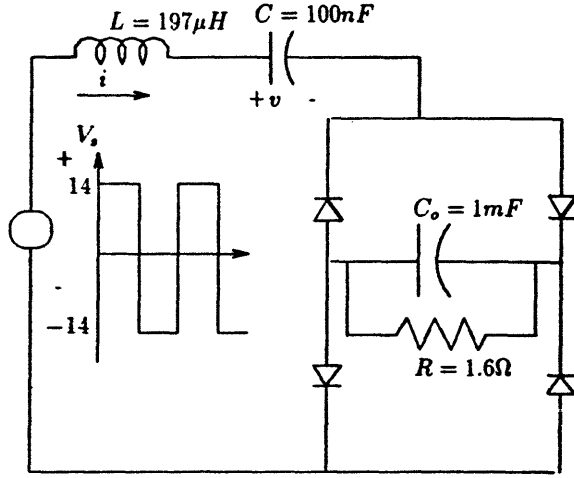
Here, $sgn(\bullet)$ and $abs(\bullet)$ are, respectively, the sign and absolute value functions.

In our analysis, we retain the fundamental frequency Fourier coefficients for i and v and the DC coefficient for v_o. This choice can be motivated by studying the converter waveforms and noting that the variables i and v exhibit predominantly sinusoidal behavior while the output voltage v_o exhibits rather slowly varying dynamical behavior. If this was not the case, more terms could be retained in the averaged model. The key steps in applying the averaging operation to the model (35) are in computing $\langle sgn(i)v_o \rangle_1$ and $\langle abs(i) \rangle_0$. These can be determined using describing function methods if i and v are considered to be sinusoidal and v_o is approximated with a constant term. With these simplifying assumptions, we find

$$\langle sgn(i)v_o \rangle_1 \approx \frac{2}{\pi}\langle v \rangle_0 e^{j\angle(i)_1} \qquad (36)$$

$$\langle abs(i) \rangle_0 \approx \frac{4}{\pi}\|\langle i \rangle_1\|. \qquad (37)$$

In order to verify the obtained average model, a simulation that compares waveforms generated by this model with waveforms of the underlying system is shown in Figure 6. As is evident from the figure, the averaged model predicts the transient behavior quite accurately. Analysis steps similar to those carried out in the previous example could be performed, but we omit the details. •

PWM Up-Down Converter In this final example, we illustrate how to refine the method of state-space averaging by including higher order terms in the Fourier series expansion (17). The converter of Figure 7 operating in continuous conduction mode can be modeled with a second order state-space model of the form

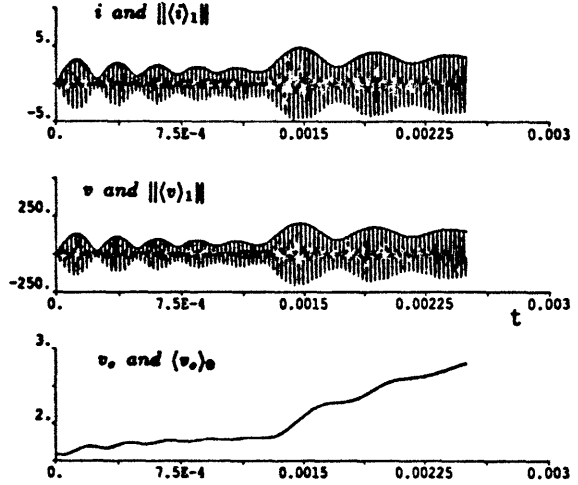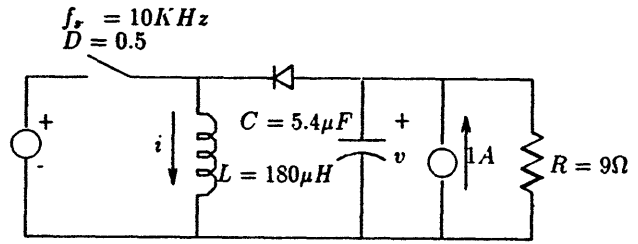$$\frac{d}{dt}x = Ax + uBx + bu + f \qquad (38)$$

Figure 7: Up-Down Converter

where the variable u takes the values 0 and 1 which correspond to the instaneous switch position. For nominal PWM operation at the fixed frequency $f_s = \omega_s/2\pi$, the state-space averaged model can be obtained by applying the one-cycle averaging operation $\langle \bullet \rangle_0$ to the model (38). A refinement of the state-space averaged model can be obtained by considering an additional term in the series (17) that corresponds to the fundamental component of the ripple. For this, we consider the application of both $\langle \bullet \rangle_0$ and $\langle \bullet \rangle_1$ to the model (38). The result is

$$\frac{d}{dt}\langle x \rangle_0 = A\langle x \rangle_0 + B(\langle x \rangle_0\langle u \rangle_0 + \langle x \rangle_1\langle u \rangle_{-1} + \langle x \rangle_{-1}\langle u \rangle_1) + b\langle u \rangle_0 + f$$

$$\frac{d}{dt}\langle x \rangle_1 = -j\omega_s\langle x \rangle_1 + B(\langle x \rangle_1\langle u \rangle_0 + \langle x \rangle_0\langle u \rangle_1) + b\langle u \rangle_1.)(39)$$

Note that the rule (22) is used to approximate quantities like $\langle xu \rangle_0$ and $\langle xu \rangle_1$. For open-loop operation, $\langle u \rangle_0$ and $\langle u \rangle_1$ are constant, and so the model (39) is linear and time-invariant in this case. A simulation of an open-loop transient is shown in Figure 8. The figure compares the inductor current waveform of the actual circuit, the inductor current waveform of
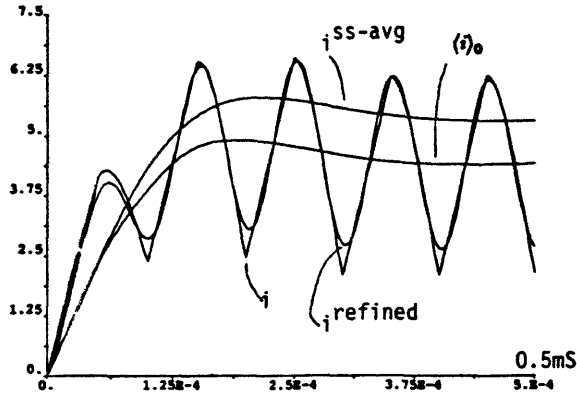
6

Figure 8: Comparison of Refined State-Space Averaged Model with Traditional State-Space Averaged Model

the state-space averaged model, $\langle i \rangle_0$ which is the dc component of the inductor current of the refined model (39), and an inductor current waveform reconstructed from the refined averaged model determined by

$$i(t) = \langle i \rangle_{-1}(t)e^{-j\omega_s t} + \langle i \rangle_0(t) + \langle i \rangle_1(t)e^{j\omega_s t}. \qquad (40)$$

The switching frequency has been selected to be relatively low so that the ripple is emphasized. As can be seen from the figure, the additional term in (39) significantly decreases the error between the waveform of the averaged model and the underlying system. Evidently, it is possible to include more terms in the Fourier series representation to further decrease approximation error.

. The refined averaged model is especially useful for analysis and control design in the case where ripple is not small. For instance. the eigenvalues of an equivalent continuous time model derived from an exact sampled-data model for the present example can be determined to be

$$\lambda_{1,2} = \frac{1}{T}log(\lambda_{1,2}\{\Phi(T)\}) = (-1.029 \pm j1.328) * 10^4.$$

Note that $\Phi(T)$ is the transition matrix for (38). In comparison, the eigenvalues of the state-space averaged model are given by

$$\lambda_{1,2}^{ss-avg} = (-1.029 \pm j1.230) * 10^4$$

while those of the refined model are given by

$$\begin{aligned} \lambda_k^{refined} &= (-1.029 \pm j1.325) * 10^4, \\ &\quad (-1.029 \pm j5.149) * 10^4, \\ &\quad (-1.029 \pm j7.707) * 10^4. \end{aligned}$$

One pair of the eigenvalues of the refined model is seen to approximate the eigenvalues of the underlying system much more closely than those of the usual state-space averaged model. ●

5 Conclusions

A new approach to averaging in power electronic circuits has been introduced, and the method has been seen to be useful

in analyzing resonant-type converters. Further, the approach offers refinements to the theory of state-space averaging that permit ripple estimates and offers a framework for analysis and design when "small ripple" conditions do not hold. The method may find applications in simulation as well as design since it is considerably easier to simulate an averaged model than a switched model.

A Time-Varying Frequency

As briefly discussed in Section 3, the analysis based on (17) and (18) is valid if ω_s is constant. In the case where the frequency $\omega_s(t)$ is time varying, it is appropriate to consider an instantaneous phase function defined via

$$\frac{d}{dt}\theta(t) = \omega_s(t). \qquad (41)$$

In this framework, the Fourier analysis should be performed with respect to the basis functions $\{e^{jk\theta(t)}\}$ for $\theta(t)$ in some interval $(\theta_1 - 2\pi, \theta_1]$ rather than the basis $\{e^{jk\omega_s t}\}$. The time interval for the analysis now depends on the instantaneous phase function in the following way. Define $T(t)$ to be the duration of time so that the phase function varies by exactly 2π on the interval $(t - T(t), t]$. That is, for a particular time t_1, $T(t_1)$ is defined by

$$\begin{aligned} \theta_1 &= \theta(t_1) \qquad &(42) \\ \theta_1 - 2\pi &= \theta\{t_1 - T(t_1)\}. \qquad &(43) \end{aligned}$$

Now for the interval $(t - T(t), t]$, the natural generalization of (17) is

$$x(t - T(t) + s) = \sum \langle x \rangle_k(t)e^{jk\theta(t-t(T)+s)} \qquad (44)$$

for $s \in (0, T(t)]$. In this case, the Fourier coefficients $\langle x \rangle_k(t)$ need to be defined via

$$\begin{aligned} \langle x \rangle_k(t) &= \int_{\theta(t)-2\pi}^{\theta(t)} x\{s(\theta)\}e^{-jk\theta}\, d\theta \\ &= \int_{t-T(t)}^{t} x(s)e^{-jk\theta(s)}\omega(s)\, ds \\ &= \int_0^{T(t)} x(t - T(t) + s)e^{-jk\theta(t-T(t)+s)} * \\ &\qquad\qquad \omega(t - T(t) + s)\, ds \quad (45) \end{aligned}$$

where $s(\theta)$ in the first line of (45) represents a local inverse map from phase to time. An easy calculation performed after changing the variable of integration in (45) by $\sigma = T(t) - s$ yields

$$\begin{aligned} \frac{d}{dt}\langle x \rangle_k(t) = &\; x\{t - T(t)\}e^{-jk\theta(t-T(t))}\omega_s\{t - T(t)\}\dot{T}(t) + \\ &\int_0^{T(t)}\{\dot{x}(t - \sigma)e^{-jk\theta(t-\sigma)}\omega_s(t - \sigma) + \\ &\{\dot{\omega}_s(t - \sigma) - jk\omega_s^2(t - \sigma)\}x(t - \sigma)e^{-jk\theta(t-\sigma)}\}d\sigma. \\ &\hspace{10cm} (46) \end{aligned}$$

This formula is equivalent to

$$\begin{aligned} \frac{d}{dt}\langle x \rangle_k(t) = &\; x\{t - T(t)\}e^{-jk\theta(t-T(t))}\omega_s\{t - T(t)\}\dot{T}(t) + \\ &\langle \dot{x} \rangle_k(t) + \langle(\frac{\dot{\omega}_s}{\omega_s} - jk\omega_s)x \rangle_k(t). \quad (47) \end{aligned}$$

7

Another simple calculation yields

$$\frac{d}{dt}T(t) = 1 - \frac{\omega_s(t)}{\omega_s\{t - T(t)\}}. \qquad (48)$$

It is now clear that for the case where ω_s is constant, (47) reduces to (20). Furthermore, for slowly varying $\omega_s(t)$, the last term in (47) is well approximated by $-jk\omega_s\langle x\rangle_k$. The term $x\{t - T(t)\}e^{-jk\theta\{t-T(t)\}}\omega_s\{t - T(t)\}\dot{T}(t)$ is also guaranteed to be small if $\omega_s(t)$ is slowly varying since $\dot{T}(t)$ is given by (48).

Another important consequence of the formula (47) is that there is no direct feedthrough term into $\langle x\rangle_k(t)$ from $\omega_s(t)$. Hence, in the case where the frequency $\omega_s(t)$ undergoes a step change, we observe no step (or impulsive) behavior in $\langle x\rangle_k(t)$. This is of interest in the examples based on resonant converters.

References

[1] R.D. Middlebrook and S. Cuk, "A General Unified Approach to Modeling Switching Power Converter Stages," IEEE PESC Record, 1976, pp. 18-34.

[2] R. W. Brockett and J. R. Wood, "Electrical Networks Containing Controlled Switches," Addendum to IEEE Symposium on Circuit Theory, April 1974.

[3] R. W. Erickson, S. Cuk, and R. D. Middlebrook, "Large-Signal Modelling and Analysis of Switching Regulators," IEEE PESC Record, 1982, pp. 240-250.

[4] G.C. Verghese, M.E. Elbuluk, and J.G. Kassakian, "A General Approach to Sampled-Data Modeling for Power Electronic Circuits," IEEE Trans. Power Electronics, pp. 76-89, April 1986.

[5] V. Vorperian and S. Cuk, "Small Signal Analysis of Resonant Converters," IEEE PESC Record, 1983, pp. 269-282.

[6] P.T. Krein, J. Bentsman, R.M. Bass, and B.C. Lesieutre, "On the Use of Averaging for the Analysis of Power Electronic Systems," IEEE PESC Record, 1989, pp. 463-467.

[7] R. Oruganti and F.C. Lee, "State Plane Analysis of Parallel Resonant Converter," IEEE PESC Record, 1985, pp. 56-73.

[8] Oruganti, Yang, and Lee, "Implementation of Optimal Trajectory Control of Series Resonant Converter," IEEE PESC Record, 1987, pp. 451-459.

[9] J.G. Kassakian, M.F. Schlecht, and G.C. Verghese, Principles of Power Electronics, Addison-Wesley, 1989.

[10] M. Vidyasagar, Nonlinear Systems Analysis, Prentice-Hall, 1978.

[11] B. van der Pol, "Forced Oscillations in a Circuit with Nonlinear Resistance (Reception with Reactive Triode)," The London, Edinburgh, and Dublin Philosophical Magazine and Journal of Science, vol. 3, 1927, pp. 65-80. Also reprinted in Selected Papers on Mathematical Trends in Control Theory, R. Belman and R. Kalaba, eds., Dover Publications, Inc., NY, 1964.

[12] N.N. Bogoliubov and Y.A. Mitropolsky, Asymptotic Methods in the Theory of Nonlinear Oscillations, Hindustan Publishing Corp., Delhi, India, 1961.

[13] A. Gelb and W.E. Vander Velde, Multiple-Input Describing Functions and Nonlinear System Design, McGraw-Hill Book Co., 1968.

[14] A.R. Bergen and R.L. Franks, "Justification of the Describing Function Method," SIAM J. Control, vol. 9, no. 4, Nov. 1971.